NREL
NATIONAL RENEWABLE ENERGY LABORATORY

ZnMgO by APCVD Enabling High-Performance Mid-Bandgap CIGS on Polyimide Modules

October 2009 — October 2010

Lawrence Woods
Ascent Solar Technologies, Inc.
Littleton, Colorado

NREL is a national laboratory of the U.S. Department of Energy, Office of Energy Efficiency & Renewable Energy, operated by the Alliance for Sustainable Energy, LLC.

Subcontract Report
NREL/SR-5200-51379
April 2011

Contract No. DE-AC36-08GO28308

NREL
NATIONAL RENEWABLE ENERGY LABORATORY

ZnMgO by APCVD Enabling High-Performance Mid-Bandgap CIGS on Polyimide Modules

October 2009 — October 2010

Lawrence Woods
Ascent Solar Technologies, Inc.
Littleton, Colorado

NREL Technical Monitor: Brian Keyes
Prepared under Subcontract No. NEU-0-99010-02

National Renewable Energy Laboratory
1617 Cole Boulevard
Golden, Colorado 80401
303-275-3000 • www.nrel.gov

Subcontract Report
NREL/SR-5200-51379
April 2011

Contract No. DE-AC36-08GO28308

Cover Photos: (left to right) PIX 16416, PIX 17423, PIX 16560, PIX 17613, PIX 17436, PIX 17721

Printed on paper containing at least 50% wastepaper, including 10% post consumer waste.

Introduction

Ascent Solar Technologies (AST) has recently begun producing lightweight and flexible photovoltaic modules to address emerging building-integrated photovoltaic (BIPV), electronic-integrated photovoltaic (EIPV), transportation and space related PV markets. AST's baseline PV technology primarily consists of typical low-bandgap $CuInGaSe_2$ (CIGS) with a CdS emitter (buffer) layer, and using roll-to-roll (R-2-R) processing on a polyimide substrate that enables monolithic integration of modules. This Pre-Incubator project was designed to increase the "real world" CIGS based photovoltaic module performance and decrease the Levelized Cost of Energy (LCOE) of systems utilizing those modules compared to our traditional CIGS based photovoltaic modules. This will be enabled by a) increasing the CIGS bandgap and b) developing better matched device finishing layers to the mid-bandgap CIGS based photovoltaics; including window and buffer layers (and eventually the TCO). Our approach to replace the traditional device finishing layers is to use metal-oxide alloys such as ZnMgO deposited by atmospheric pressure chemical vapor deposition in a roll-to-roll configuration. Furthermore, elimination of the small amount of Cd in our product will reduce costs and enable markets where Cd is either currently restricted or is being considered for restricting Cd-bearing materials.

Background

Typical high-efficiency CIGS devices utilize a low-bandgap (approx. 1.15 eV) CIGS solar absorber layer and a CdS based buffer layer adjacent to the solar absorber. The low-bandgap of typical CIGS devices results in module power losses (lower efficiency) due to two important factors: (1) High current modules resulting in high joule heating or I^2R power losses, and (2) Large negative voltage and power temperature coefficients resulting in significantly reduced power at nominal operating temperatures of 40 to 80 ºC. This latter factor is a market barrier for structurally integrated modules (ex. BIPV) and structurally applied (ex. BAPV, EIPV, etc.) modules based on CIGS solar absorbers as it impedes the realization of high-efficiency flexible modules. Higher bandgap CIGS solar absorbers would significantly reduce these loss factors and our internally module modeling indicates that module performance could be increased by as much as 10 to 30% over the lower bandgap module at nominal operating temperatures. However research to date shows that the CIGS device (small-area) efficiency *decreases* as the band-gap is increased to more desirable single-junction levels (1.35 to 1.45 eV). The cause of the diminished performance is attributed to two theories: (1) Deep defect levels becoming more mid-gap with increasing bandgap and thus becoming more effective recombination centers,[1] and (2) traditional device layers window and buffer layers are not well matched to the wider-bandgap CIGS (higher Ga) solar absorber. [2,3,4] The former has limited mid-bandgap CIGS efficiencies to about 13% (small-area) on high temperature glass substrates when using traditional window and buffer (CdS) layers.[1] Regarding the latter, a better matched buffer layer may enable better mid-bandgap CIGS performance over CdS buffers due to better conduction band line-up and a reduction in interface recombination. Furthermore, the Cd in the CdS layer is a market barrier in some countries (ex. Japan), and as such results in an indirect cost increase. In addition, costs for proper hazardous material handling at the manufacturing facility and waste removal and treatment of CdS further increases the costs associated with this layer. Thus there is room for considerable improvements in traditional CIGS devices as they relate to module performance, especially in structurally integrated markets.

Project Approach

The approach of this Pre-Incubator project was to produce mid-bandgap CIGS solar absorbers using multi-source co-evaporation on molybdenum coated polyimide substrates, and optimize the CIGS composition in the bandgap range of 1.35 to 1.45 eV. Anticipated variables include the final Cu/III ratio, Ga/III ratio, sodium content, and the substrate heater temperature. As planned, we initially used a small bell jar co-evaporation system with a stationary substrate configuration for the CIGS depositions, and later in the program migrated to a larger Roll-to-Roll (R-2-R) co-evaporation system from the pilot line. The R-2-R system provided more CIGS material and more uniform CIGS compositions as needed for the buffer layer development and good comparison with buffer layer controls (with CdS). The R-2-R system was also used for CIGS depositions that further incorporated sodium (Na) into the mid-bandgap solar absorber make-up. Finally, the R-2-R system was used in AST's internal development that produced novel CIGS based mid-bandgap alloys and that were leveraged for use with the novel metal-oxide buffer layers being developed under this project.

The approach to produce non-CdS based window and buffer layers for the mid-bandgap solar absorbers was to utilize atmospheric pressure chemical vapor deposition (APCVD) as a 'gentle' technique (not damaging to CIGS surface) in a belted (amenable to R-2-R) deposition system to develop metal-oxides such as ZnMgO for use as the window and buffer layer with mid-bandgap CIGS. The proposed mid-bandgap CIGS device layers in cross-section versus the baseline low-bandgap CIGS device layers are illustrated in Figure 1 below.

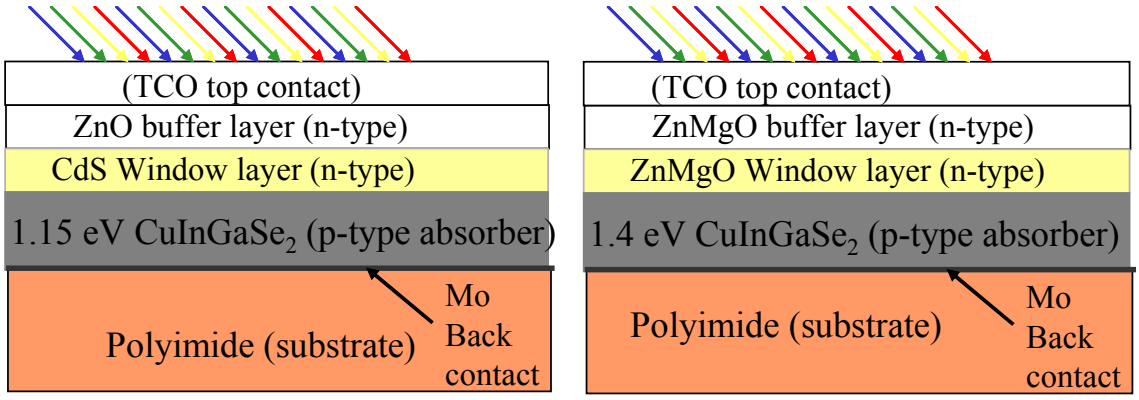

Figure 1 - The proposed mid-bandgap CIGS device layers in cross-section (right) versus the baseline low-bandgap CIGS device layers (left).

Several process variables related to the fabrication of the metal-oxide buffer layer and device junction were identified and planned for testing during the program. The variables have been categorized below, and their anticipated effect on the buffer layer material is noted.

- CIGS surface preparation and/or pre- treatment (Pre-CVD deposition)
    - Clean, passivate, create buried homojunction

- APCVD Buffer Layer deposition parameters: example ZnMgO: Zn conc., Mg conc., Zn/Mg (alloy) ratio, metals/oxygen ratio, substrate temperature, film thickness, dopant level.
    - Resistivity, stoichiometry, transmission, and composition.
- Post APCVD Buffer Layer Annealing
    - Junction Cross-diffusion, layer crystallinity, resistivity and transmission, passivation of CIGS.
- Post Device Annealing
    - Same as above, but this now includes i-ZnO and TCO and their interfaces.

Summary of Program Goals and Objectives

The overall goal of the program was to develop the technology for higher performance mid-bandgap (1.35 eV to 1.45 eV) CIGS based photovoltaics on **polyimide** substrates that utilize metal-oxide buffer/window layers (no CdS) as deposited by non-surface damaging APCVD.

The Technical Improvement Opportunities (TIO's) addressed in the project are: (1) Absorber (CIGS), and (2) Cells and Contacts (window and buffer layers).

The small area (1 cm^2) device efficiency goals for the novel mid-bandgap devices on **polyimide** substrates were as follows:

- 6% eff. by month 6
- 8% eff. by month 9
- 9% eff. by month 12

Key objectives of the development effort enabling progress toward these performance goals were as follows:

- Produce mid-bandgap CIGS solar absorbers of about 1 micron thickness using multi-source roll-to-roll (R-2-R) co-evaporation on molybdenum coated polyimide substrates, and optimize the CIGS composition (Eg = 1.35 to 1.45 eV) for higher Open Circuit Voltage (Voc) and lower temp. coefficients.
    - Critical success factor related to KPPs: Bandgap > 1.35 eV (reduced Indium), Thickness of about 1 micron (reduced materials).
- Replace CdS and utilize R-2-R Atmospheric Pressure Chemical Vapor Deposition (APCVD) to develop metal-oxides such as ZnMgO for use as the window and buffer layer with mid-bandgap CIGS.
    - Critical success factor related to KPPs: Higher performance device at nominal operating temperatures (vs. low bandgap), Cost of metal-oxide buffer < cost of CdS

Accomplishments of Performance Milestones and/or Deliverables

Several milestones were planned as a check on the projects progress. These milestones are listed in Table 1 below along with their due dates and final status.

Table 1 – Planned milestones, due dates, and final status.

Milestone	Month	Summary Status
Task 3.1 Fabricate Hardware Baseline	1	On time. Accepted at NREL
Task 3.2 Mid-bandgap (Eg >1.35eV) CIGS samples fabricated	1	On time. Mid-bandgap development was ongoing throughout the remainder of program.
Subtask 3.2.1 Mid-bandgap (Eg>1.35eV) CIGS with Na samples fabricated	3	On time. Mid-bandgap development with Na was ongoing throughout the remainder of the program.
Subtask 3.2.2 Mid-bandgap (Eg>1.35eV) thin < 2 μm thick) CIGS samples fabricated	5	On time. Mid-bandgap development with thinner absorbers was ongoing throughout the remainder of the program.
Task 3.3 APCVD Metal-oxide films fabricated with targeted composition, and optical properties.	2	On time. Metal-oxide depositions were ongoing throughout the remainder of the program.
Subtask 3.3.1 Surface pretreatment effectiveness determined	4	On time. Surface pretreatments were ongoing throughout the remainder of the program.
Subtask 3.3.2 Doping effectiveness determined	6	On time. Doping and alloying were ongoing throughout the remainder of the program.

The baseline device deliverable was sent in before the end of the first month of the program, and was been accepted by NREL. Toward the end of the 2nd quarter (6 months), the 6 month 6% eff. device deliverable was sent in to NREL for performance verification and accepted. Toward the end of the 3rd quarter (9 months), the 9 month 8% eff. and the 12 month 9% eff. device deliverables were sent in to NREL for performance verification and accepted. By the 11th month of the program, a 12% efficient device (as measured by AST) on polyimide substrates was produced using a mid-bandgap CIGS based alloy and metal-oxide buffer and finishing layers (no CdS). The bandgap of this device was determined to be about 1.40 eV as determined by the examination of the absorber band edge from quantum efficiency measurements.

Detailed Progress on Key Performance Parameters (Project Results)

The mid-bandgap CIGS deposition process on the temperature restricting polyimide substrates was developed and optimized through-out the program, and overall there have been 23 large multi-variable experiments performed using the mid-bandgap CIGS with APCVD buffer layers. A summary of the all the experimental variables tested during the program are summarized in Table 2.

Table 2 – Summary of all the experimental variables for the metal-oxide buffer layer development on mid-bandgap CIGS and organized according to category.

CIGS Solar Absorber	CIGS Surface Treatments	APCVD Alloyed ZnO Deposition	Post-Anneal
Low Cu/(In+Ga) ratio	None	Substrate Temp.	None
Mid Cu/(In+Ga) ratio	#1	Metals/O2 ratio	Anneal #1
High Cu/(In+Ga) ratio	#2 (1X and 2X conc.)	Metals conc.	
CIGS Surface composition variations.	#3	Metals Alloy %	
With Sodium	#1 or #2, and #3	Metals type	
R-2-R CIGS	#1 and/or #3		
R-2-R CIGS with Sodium	#4, #5, #6, #7 or #8		
R-2-R CIGS alloy With Sodium	Pre Anneal #1		
R-2-R CIGS alloy Without Sodium	Pre Anneal #2		

CdS buffer layer controls devices were fabricated and tested for all experiments and mid-bandgap solar absorbers. In all experiments each experimental buffer layer sample and CdS/CIGS control were finished into approximately twelve individual 1 cm^2 small area devices, then prepped (back contact access) and tested using simulated AM1.5 light IV testing. In many cases, quantum efficiency (QE) measurements were performed to assess the device spectral response and effective bandgap from the long wavelength cut-off. The composition of the mid-bandgap CIGS solar absorber was determined using x-ray fluorescence measurements, and was also used as a guide to achieve targeted bandgaps when used in conjunction with published data on CIGS bandgap versus Ga/(In+Ga) ratio.

During the first quarter of the project all CIGS depositions were accomplished in a small bell jar with a stationary substrate configuration. Prior to the CIGS sample fabrication, the maximum substrate heater temperature was approx. determined by visual and mechanical inspection of the substrate after several calibration runs. The CIGS produced for these early experiments had Ga/III ratios in the range of 0.5 (Eg > 1.3 eV) to 0.6 (Eg > 1.35 eV). Some of the primary variables tested during the first quarter were the Cu/III ratio of the mid-bandgap CIGS, the effect of pre-treatments to the CIGS surface, and the substrate temperature during the APCVD metal-oxide deposition. No sodium was incorporated into the solar absorber during these experiments and the primary metal-oxide under consideration was ZnMgO. The Mg/(Zn+Mg) flow ratio was

fixed at a relatively high value during these initial experiments. The results from one experiment is given below, and represents the best performance during the first quarter.

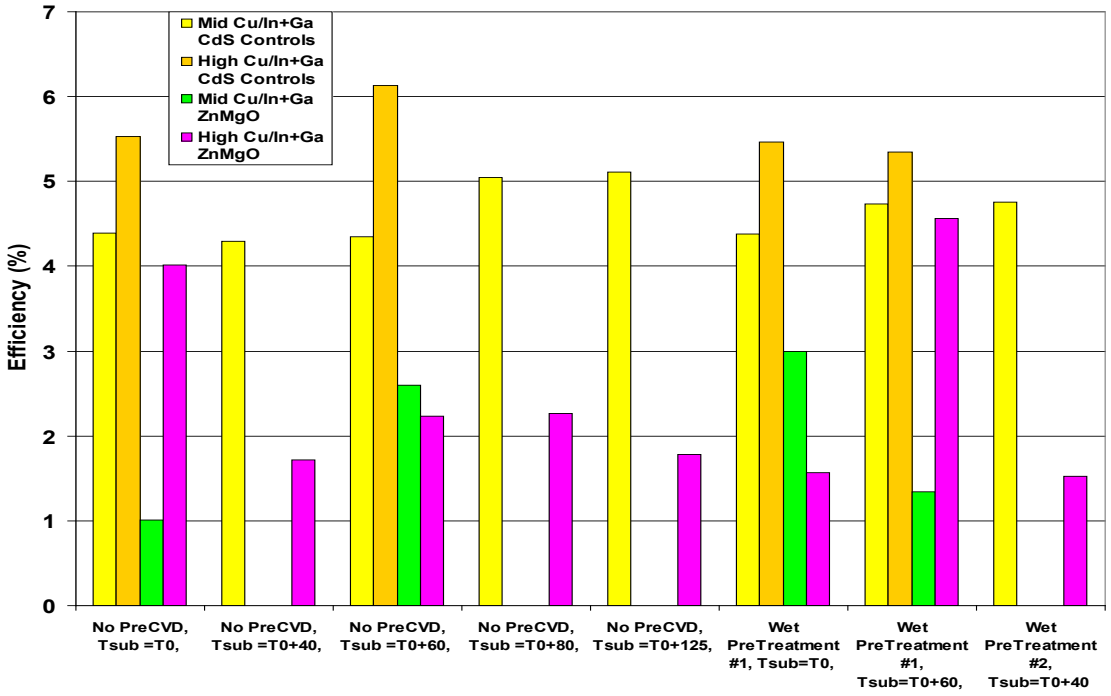

Figure 2 – Example of device efficiency results from ZnMgO/CIGS based devices (and CdS controls) with CIGS bandgap > 1.4 eV (no NaF). Best devices eff. (Top).

Device performance results from these initial experiments yielded a best experimental (ZnMgO buffer) small-area device efficiency of 4.5%, (at STC) and utilized a CIGS pretreatment, while the best CdS/CIGS control tested at 6% eff. Voc's follow eff. (not shown), higher than low-bandgap CIGS devices. The best Voc's were near 700 mV on controls, and near 600 mV on experimental devices**.** These best experimental and control samples also had the lower Ga/III ratio (Eg > 1.3), and higher Cu/III ratio, which is not indicated in the Figure.

One particular area of concern was identified during this first quarter and as a result of x-ray photoemission spectroscopy (XPS) analysis of a ZnMgO film deposited by the belt APCVD process. It was found that the Mg/(Zn+Mg) ratio varied considerably as a function of film depth, presumable due to different Zn and Mg Precursor reaction rates as the substrate traverses under the injector head. The XPS profile through the film is given in Figure 3 below. The XPS analysis was performed by Dr. Glenn Teeter at the National Renewable Energy Laboratory (NREL). The profile shows that the Zn and Mg concentrations are oppositely correlated and with Zn peaking at the beginning and ending of the film, and Mg peaking in the middle of the film. The oxygen profile also seems to peak in the middle of the film, though this variation is much more subtle. The repercussions of this type of profile were not immediately clear, but the ZnMgO design strategy was to match or slightly exceed the conduction band energy of the mid-bandgap CIGS solar absorber layer at the ZnMgO/CIGS heterointerface (similar to the CdS/low-

bandgap CIGS band line-up). Earlier absorption spectroscopy (not shown - prior to this program) showed that the ZnMgO did not have a sharp band edge, potentially now attributable to the non-uniform compositional profile, but with an ill-defined bandgap in the range of 3.3 to 3.6 eV. Thus, indication is that we will have a mostly ZnO composition adjacent to the mid-bandgap CIGS absorber. In an effort to determine if non-uniform buffer layer bandgap profiling would be problematic for the mid-bandgap CIGS devices, then device modeling was performed by Dr. Kanevce at NREL using commercial device physics based simulation software. This modeling is described in a separate section below and was ongoing throughout the majority of the program. Nonetheless, it was also decided to utilize other metals for alloying with the ZnO, in addition to the ZnMgO. Hereafter the alloyed metal-oxide buffer is collectively referred to as 'alloyed ZnO'.

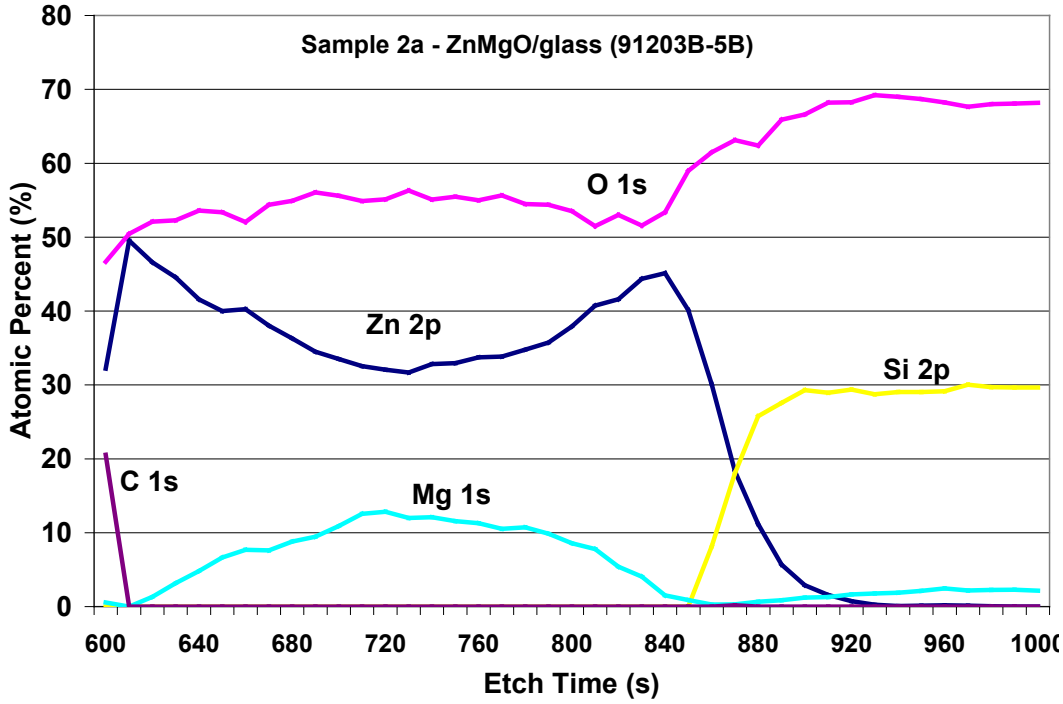

Figure 3 – XPS profile of ZnMgO film on a glass slide.

During the 2nd quarter of the project, the mid-bandgap CIGS depositions shifted to the larger roll-to-roll (R-2-R) depositions toward the latter part of the quarter. This enabled better substrate temperature control and more plentiful mid-bandgap CIGS solar absorber material for the buffer layer device experiments. As a part of the 2nd quarter experiments several mid-bandgap CIGS solar absorber 'types' were tested, including three levels of Cu/III ratio (low, medium, and high), sodium additions, CIGS surface composition variations, and combinations thereof. In addition, mid-bandgap CIGS and CIGS alloys were produced from a roll-to-roll deposition system and tested with the APCVD buffer layer variations. Three different CIGS surface treatments were also tested. Regarding the APCVD deposition itself, variations in the alloyed ZnO content and

substrate temperature were tested. A summary of the results grouped according to mid-bandgap absorber layer type are as follows:

- Small Bell Jar Stationary Substrate Mid-Bandgap CIGS (no sodium addition)
    - Alloyed metal oxide buffer layer were better than some of the CdS buffer layer controls.
    - Best devices tended to be samples with a CIGS pre-treatment (#2)
    - Samples with a medium level of Cu/III performed best.
    - Overall efficiencies were still less than 5% eff.
- R-2-R Mid-Bandgap CIGS with sodium.
    - The best CdS/mid-bandgap CIGS was over 9% eff. (Eg. = 1.35 eV)
    - Alloyed ZnO buffer layer samples all tested out with much lower efficiencies (best 3% eff.)
    - The best alloyed ZnO buffer sample utilized a CIGS pre-treatment (#3-2 or #2 + #3-0) and a higher level of alloying with the ZnO.
- R-2-R Mid-Bandgap CIGS alloy without sodium (from Internal Development)
    - The best CdS/mid-bandgap CIGS was measured to be over 8% eff. and Voc = 0.57 V (Eg = 1.35 eV)
    - Alloyed ZnO buffer layer samples tested out with higher efficiencies than controls, best over 9% eff., Voc = 0.57 V (Eg = 1.35 eV). Best Voc's near 600 mV
    - The best experimental sample did not utilize a CIGS pre-treatment, but some of the pre-treated samples did better than the controls as well.
    - A higher level of ZnO alloying was also found to have a significant benefit
    - Alloyed ZnO Buffer layer samples deposited at intermediate substrate temperatures performed best.
    - Devices require post-fabrication annealing to maximize performance (FF).

The device results from one experiment during the second quarter are given in Figure 4 below as an example, and some of these samples represent the best performance during the 2nd quarter.

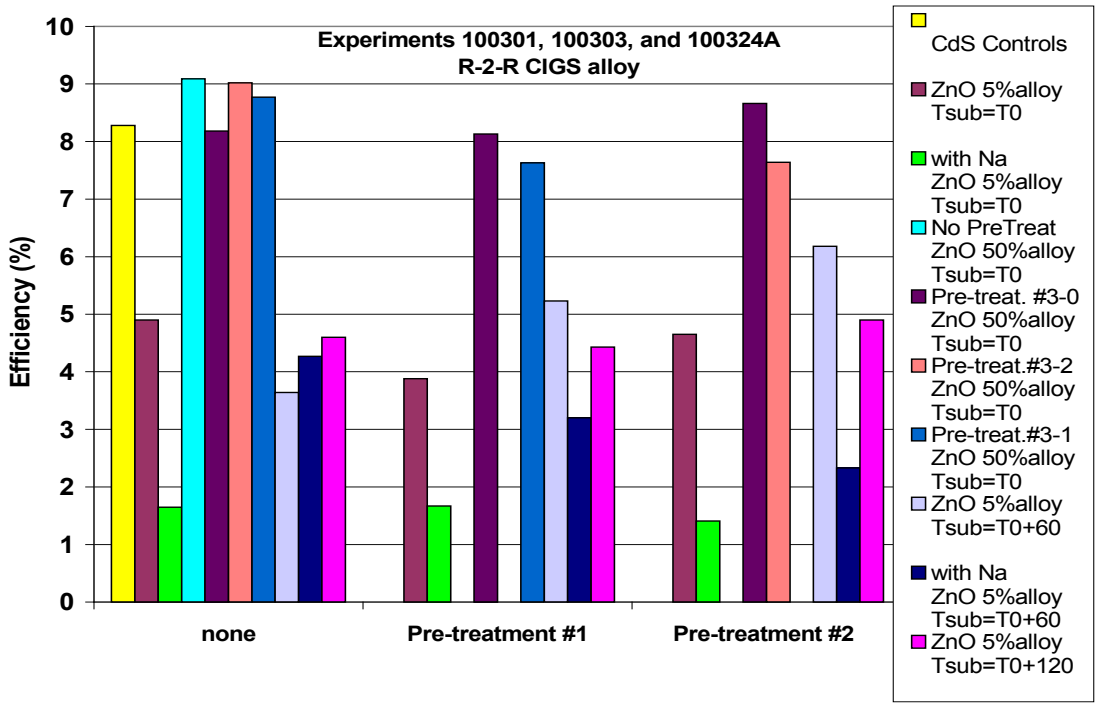

Figure 4 - Example of device efficiency results from an experiment with alloyed ZnO buffer layers (and CdS controls) and mid-bandgap CIGS alloyed based absorbers from R-2-R deposition system, no NaF. The CIGS bandgap is approximately 1.35 eV.

The primary finding during the 2nd quarter was that the Na containing mid-bandgap solar absorbers with traditional CdS buffer layers performed well and much better the alloyed ZnO based buffer layers, but the alloyed ZnO based buffer layers performed as well or better than the CdS buffer layers when no Na was incorporated into the CIGS, but overall the performance seemed to be limited to 9% eff. One other significant finding was noted during this quarter, and that is that some of the devices required proper storage to stabilize the performance. The initial indications were that that the storage ambient depended on whether or not there was sodium in the CIGS alloys.

During the 3rd quarter, the large scale experiments focused on the alloyed ZnO buffer layer development with a mid-bandgap CIGS alloy solar absorber (from internal development). The mid-bandgap CIGS alloys were obtained from a roll-to-roll (R2R) deposition system and during the 3rd quarter the program utilized material from four different runs; three of these had sodium added. In addition, several different CIGS surface treatments were tested, including several new ones (#4 - #8) in an effort to improve the device performance with the Na treated CIGS alloy. Some of the different pre-treatments were sometimes done in combination with other pretreatments. Regarding the APCVD deposition itself, variations in the ZnO alloy content, metals/oxidant ratio, and substrate temperature were tested.

In the first few experiments, the CIGS and CIGS alloy compositions with sodium (Na) were utilized to improve the device performance when using the Na containing solar absorbers. Several new pre-treatments were tested to help remove excess Na, and were tested with several

different variations in the APCVD process. An example of the device efficiency results from one of the experiments is shown in Figure 5. Some of the new pre-treatments were found to be beneficial and the ZnO alloy process variations were influential as well. One of the experimental ZnO alloy buffer layer devices was tested at close to 10% eff., the best ZnO alloy/mid-bandgap CIGS device to date, but the mid-bandgap CIGS with the CdS buffer layer tested at about 12% eff. (Eg ≅ 1.35 eV).

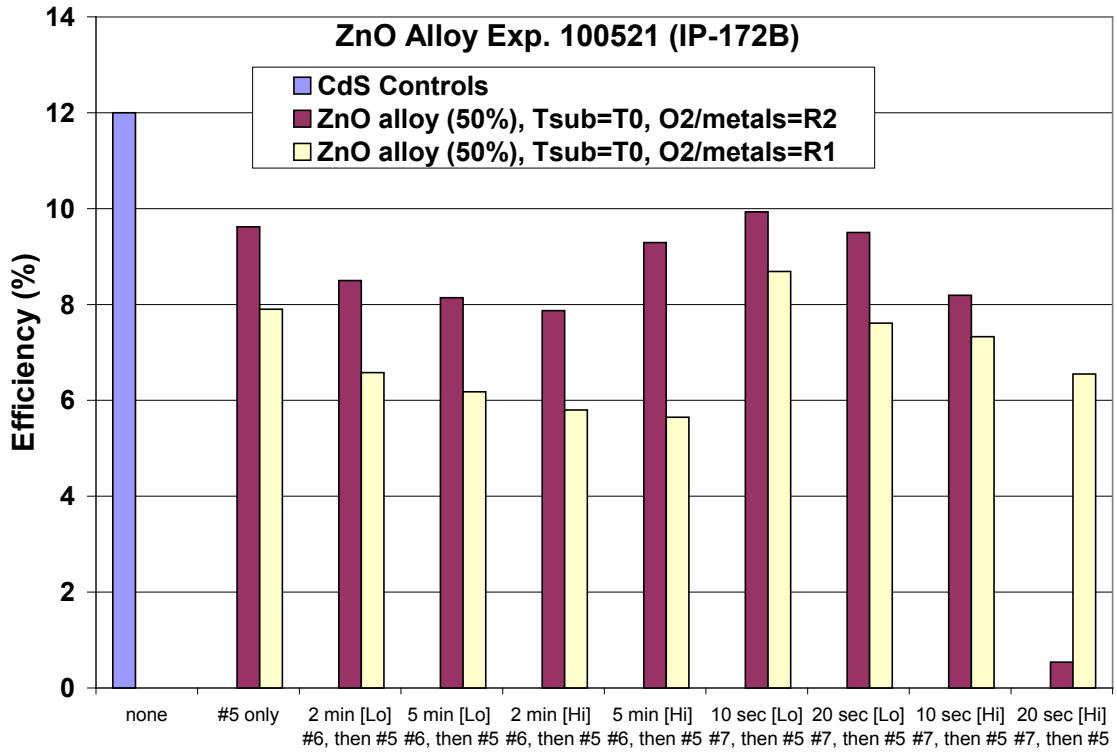

Figure 5 – Summary of Best Device Performance from ZnO alloy/mid-gap CIGS alloy based devices (with Na) and CdS buffer controls as a function of APCVD pre-treatment from exp. 100521.

Later in the 3rd quarter, another advance in the alloyed ZnO/mid-bandgap CIGS alloy performance was obtained, and the best device was measured (after light soaking) at over 11% eff. (Voc = 0.615), now performing much closer to the CdS buffer layer control which again tested at 12% eff. (Voc = 0.687). The best experimental sample utilized a pre-anneal, pre-treatment #5, and a higher ZnO alloying %. The device light IV curves from this best alloyed ZnO buffer layer and corresponding CdS buffer layer devices with the mid-bandgap CIGS alloy are shown in Figure 6. The best alloyed ZnO/mid-bandgap CIGS alloy device was submitted as a deliverable and also tested at NREL at over 11% eff. and Voc of 637 mV (after light soaking). The QE from the best device indicated a bandgap close to 1.32 eV (not shown).

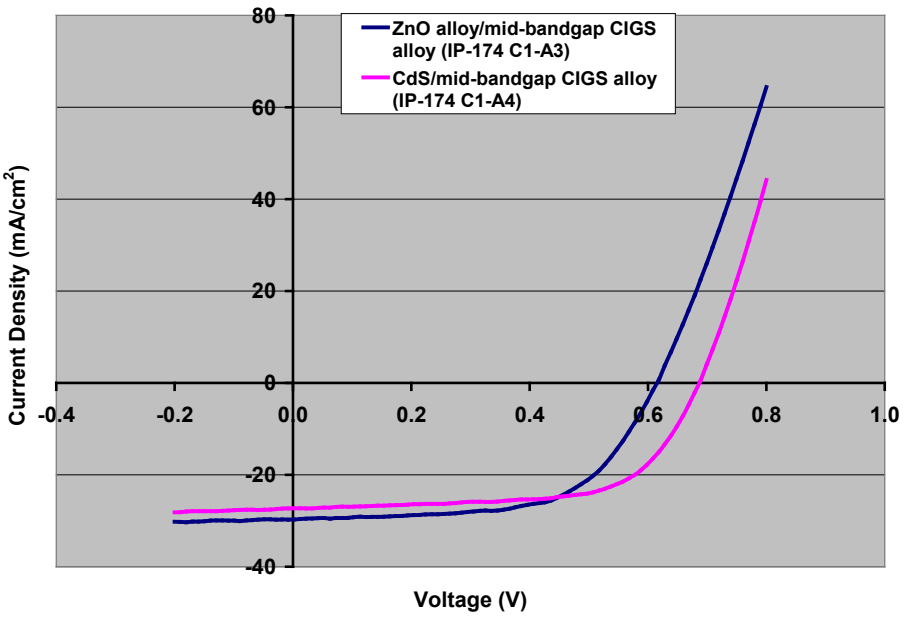

Device ID	Eff (%)	Voc (V)	Jsc (mA/cm^2)	Fill Factor
Alloyed ZnO/Mid-Bandgap CIGS Alloy (IP-174 C1-A3 - 10 min LS)	11.16	0.615	29.74	0.61
CdS/Mid-Bandgap CIGS Alloy (IP-174 C3 NO LS RETEST-A4)	12.15	0.687	27.29	0.65

Figure 6 – Light IV curves from an alloyed ZnO buffer with a mid-gap (1.32 eV) CIGS alloy (R-2-R) and CdS buffer controls.

Eventually, another experiment was run using the CIGS alloy **without** Na to determine if these solar absorbers would also benefit from the latest APCVD ZnO alloy deposition conditions and tested in combination with different anneals (pre- and post-sputtered i-ZnO/TCO). The best device performance from this experiment was about 9% eff., and thus equaling the performance that which was obtained in earlier experiments with the non-Na containing solar absorbers. The best alloyed ZnO/mid-bandgap CIGS alloy device from this experiment was submitted as a program deliverable and tested at NREL at over 8.5% efficient (after light soaking). The QE from the best device indicated a bandgap of about 1.35 eV (not shown).

Despite the very good mid-bandgap performance on polyimide substrates during the 3rd quarter, it can be seen from Figure 6 that the Voc and FF of the alloyed ZnO buffer were still in need of improvement and perhaps suffering from low free carrier density (buffer layer or CIGS alloy) and/or some interface recombination.

During the 4th quarter, the large scale experiments again focused on the alloyed ZnO buffer layer development with a mid-bandgap CIGS alloy solar absorber (from internal development). The mid-bandgap CIGS alloys were obtained from a roll-to-roll (R2R) deposition system and during the 4th quarter the program utilized material from a couple of different runs; all with sodium added. During this quarter, we targeted higher bandgap solar absorbers (> 1.4 eV) to be tested along with the latest pre-treatments/pre-anneals and buffer layer conditions that had produced the best results to date. Regarding the APCVD deposition itself, variations in the alloyed ZnO composition, metals/oxidant ratio, and substrate temperature were tested.

An example of the device efficiency results from one of the mid-bandgap CIGS alloy experiments (Eg ≅ 1.40 eV) is shown in Figure 7 below, which also further includes a low-bandgap (Eg ≅ 1.16 eV) baseline device for comparison. One of the experimental alloyed ZnO buffer layer devices was tested at over 12% eff., representing the best alloyed ZnO alloy/mid-bandgap CIGS device to date, and the highest bandgap. However, again the mid-bandgap CIGS with the CdS buffer layer tested out slight higher at about 13% eff. (Eg ≅ 1.40 eV). The power temperature coefficient in the temperature range of 20 to 65 °C is indicated in Figure 9.

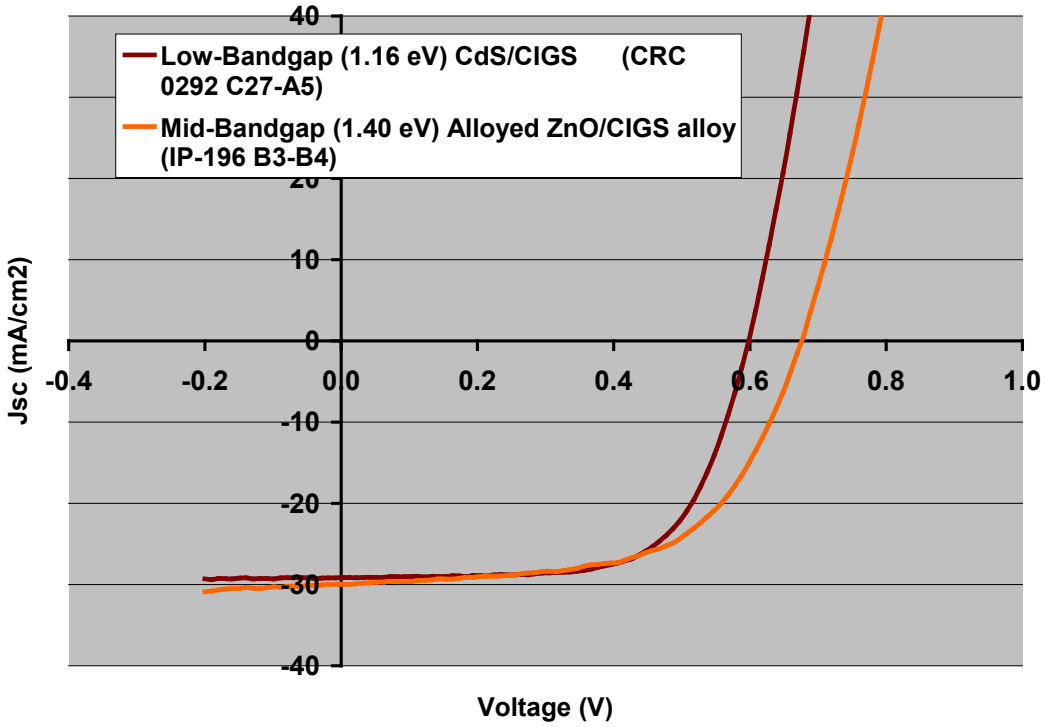

Device ID	Eff (%)	Voc (V)	Jsc (mA/cm^2)	Fill Factor
Mid- Bandgap (1.40 eV) Alloyed ZnO/CIGS alloy (IP-196 B3-B4)	12.1	0.676	30.0	0.60
Low Bandgap (1.16 eV) CdS/CIGS (CRC 0292 C27-A5)	11.6	0.598	29.1	0.66

Figure 7 – AM1.5 light IV curves of alloyed ZnO buffer layers on mid-bandgap CIGS alloy solar absorber device (1.4 eV), and low-bandgap (1.16 eV) CdS/CIGS control.

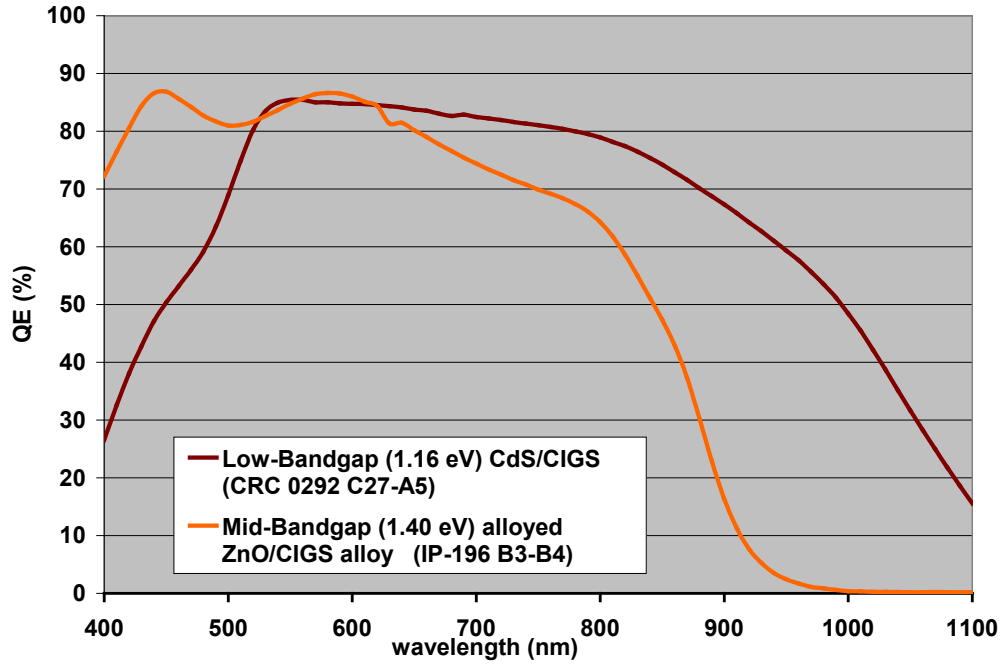

Figure 8 –QE curves of alloyed ZnO buffer layers on mid-bandgap CIGS alloy solar absorber device (1.4 eV) and Low Bandgap (1.16 eV) CdS/CIGS control.

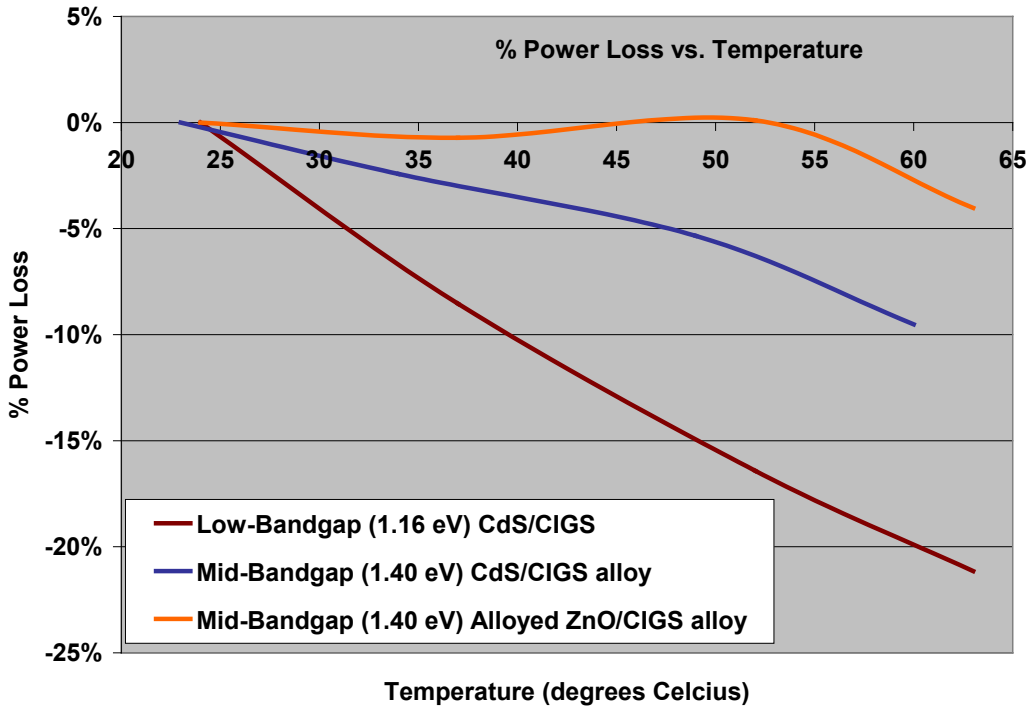

Figure 9 – % Power Loss vs. temperature for alloyed ZnO and CdS buffer layers on mid-bandgap CIGS alloy solar absorber devices, and standard CdS/CIGS low bandgap device.

Device Stability

Early in the program, the unencapsulated mid-bandgap devices with the alloyed ZnO based buffer layers showed a higher level of performance instability and light soaking sensitivity than the CdS buffer layer counterparts. The inconsistent performance initially interfered with our ability to achieve good correlation between measurements here at AST, and later measurements at NREL. It was eventually determined that the inconsistencies were largely due to our lack of experience with these types of devices, especially the effects of light soaking, and post fabrication annealing and storage conditions. Through additional testing it was first determined that the devices required light soaking at Voc (or Pmax) of at least a few minutes to maximize the device performance, and this timing sometimes varied with the ambient storage conditions. The testing also revealed that the effects of post-device annealing were highly dependent upon the processing conditions. Almost every sample generated under this program had a different processing condition, making it very difficult to determine the best annealing and storage conditions for every sample. However in general, the annealing effects seemed to depend most on whether or not the CIGS had sodium added or not and the ambient gas being used. This was also true with regard to the storage ambient. The knowledge of annealing and storage conditions effects eventually enabled very good correlation between the device performance at AST and NREL. Furthermore, the continued retesting of unencapsulated novel devices kept in the proper ambient and in the dark and at Voc, did not show any obvious degradation when considering all the potential sources for device and testing variability. Figure 10 below shows the average sample efficiency and std. deviation (12 devices each sample) over a couple of months of this storage condition. The indication is that there is a systematic variation in the average performance of all the novel buffer layer devices that also affected one of the CdS buffer layer controls. This is seen as a performance increase after a couple of weeks then a performance decrease after 10 weeks. The exception is the CdS control for the “no Na” absorber, which showed only decreased performance that is likely due to being stored in the wrong ambient (air) as the other CdS control was stored under nitrogen. The system and test variations that may affect the unencapsulated device performance include the following factors: ambient humidity during testing (not controlled), air infiltration into nitrogen cabinet (no desiccant used in sample boxes), contacts during testing, variations in light level from solar simulator (uniformity of illumination, variation after calibration), and light soaking time. Finally, almost every sample generated under this program had a different processing condition, making it very difficult to determine the best storage conditions for every sample. Thus there is some likelihood that the unencapsulated samples shown in Figure 10 are not being optimally stored. In conclusion, the data to date on the unencapsulated novel devices does not indicate any obvious degradation trends.

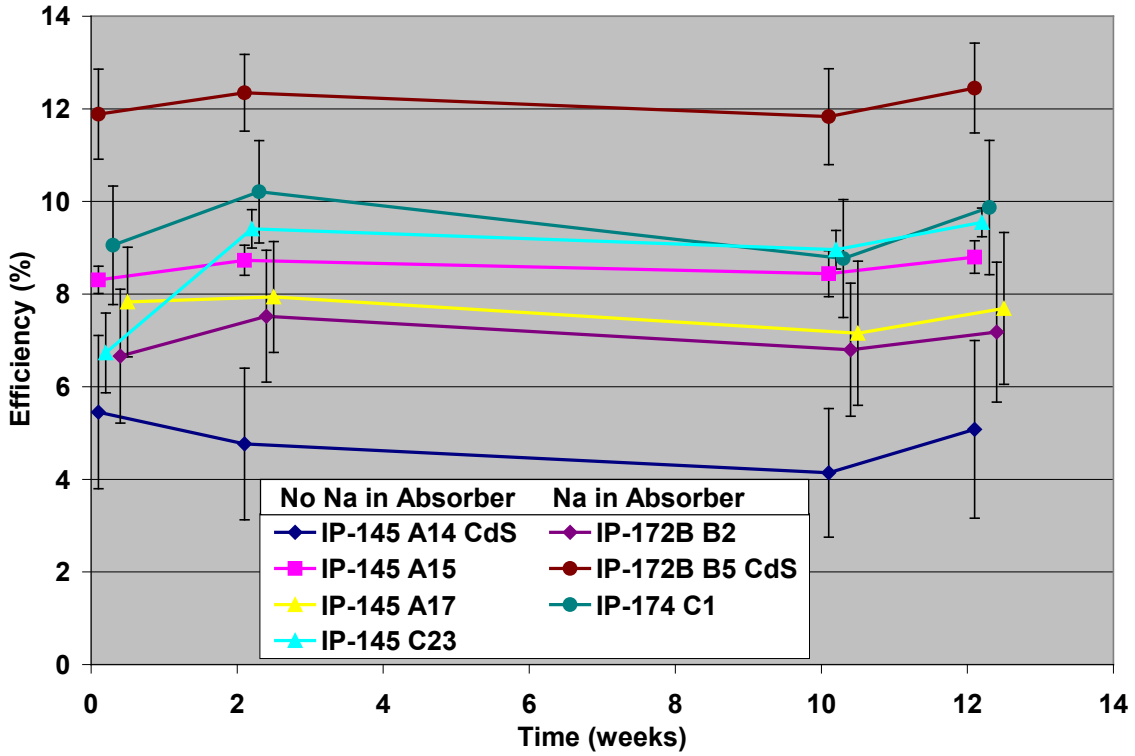

Figure 10 – Average device efficiency and std. deviation versus time in storage (dark, at Voc) from several alloyed ZnO/mid-bandgap CIGS alloy samples (approx. 12 devices each sample). Samples with CdS buffer layers instead of the alloyed ZnO are as indicated, as is the presence of sodium (Na) in the absorber (different storage ambient).

Mid-Bandgap CIGS Device Simulation Results

Device modeling and simulation was performed by Dr. Ana Kanevce at NREL (Electro-optical characterization group) using commercial device physics based simulation software in an effort to determine if non-uniform ZnMgO buffer layer bandgap profiling would be problematic for the mid-bandgap CIGS devices. The impetus for the modeling was earlier compositional profile measurements of the ZnMgO buffer layers (discussed above) that showed non-uniform Zn and Mg content through the film thickness, with Mg peaking in the middle of the film, and most likely a result of different Zn and Mg precursor reaction rates as the samples pass under the APCVD injector. The conduction band diagram for the ZnMgO/mid-bandgap CIGS material system is simulated and shown in Figure 11.

Several scenarios were modeled, and included the following variations:

- ZnMgO bandgap profile (constant vs. Gaussian),
- ZnMgO/CIGS conduction band offsets,
- ZnMgO/CIGS interface defect density,
- ZnMgO and CIGS free carrier concentrations.

In the first simulation case, the peak conduction band energy of the Gaussian profile was made to match that of the conduction band energy of the constant band profile case, but at the heterointerface there is a conduction band cliff of about 0.3 eV with the Gaussian profile, and no cliff or slight barrier with the constant band profile, similar to that of Figure 11.

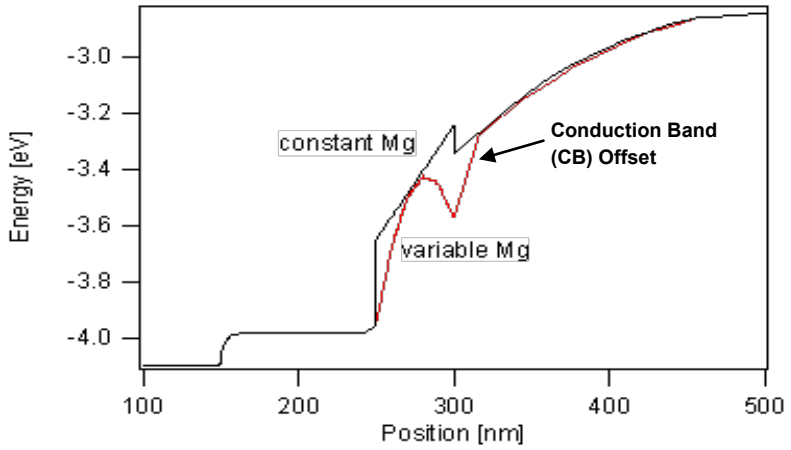

Figure 11 – Simulated Conduction band diagram at V=0 for ZnO/ZnMgO/mid-bandgap CIGS (1.45 eV) for two cases: small barrier at heterointerface and constant Mg in ZnMgO (black), and 0.3 eV cliff at heterointerface and Gaussian Mg profile in ZnMgO (red).

The effect of a ZnMgO Gaussian composition profile on the light IV curve is shown in Figure 12 below, and is plotted as a function of the defect state density at the heterointerface.

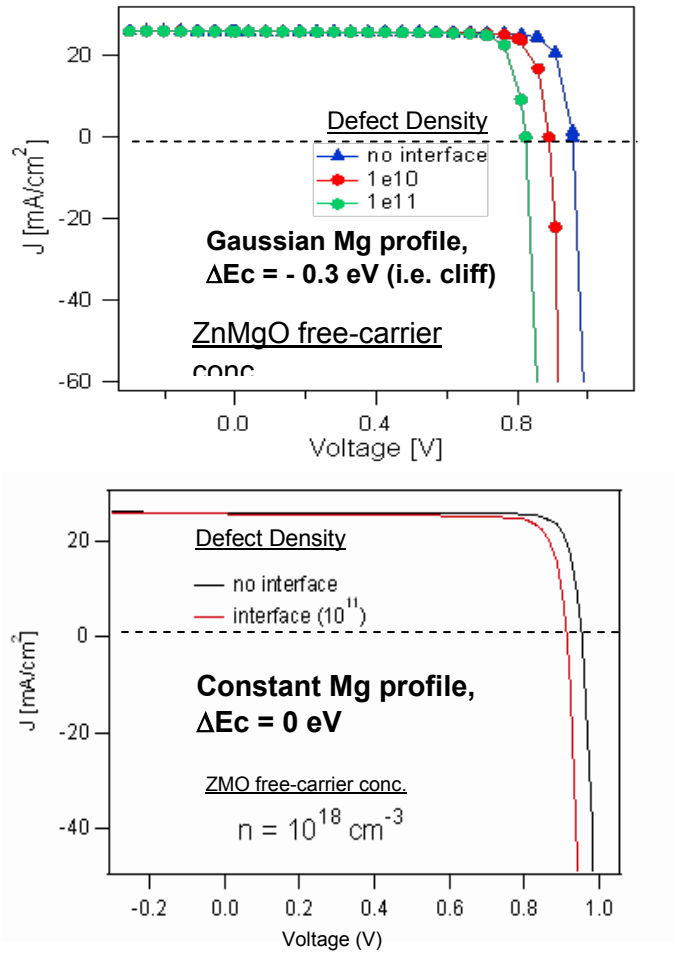

Figure 12 – Light IV device simulation results of ZnMgO (n=10^{18} cm^{-3}) with Gaussian composition profile (top) and constant profile (bottom) as a function of defect density at the heterointerface with mid-bandgap CIGS showing. (graphs have different y-scale)

In general, the simulation shows that the low Mg at CIGS interface with the Gaussian profile has a more pronounced Voc loss with increasing interface defect density up to 10^{11} cm^{-2}. This confirmed the concern with the Gaussian ZnMgO composition profile. However, additional simulations showed that the Gaussian profile appears to be beneficial when the ZnMgO free-carrier concentration is lower. This is shown in Figure 13 below as the ZnMgO free-carrier concentration is reduced to n = 10^{13} cm^{-3} for both cases. With the lower free-carrier concentration, the Gaussian profile case shows much lower Voc losses with increasing interface defect density, similar to that of the high free-carrier concentration with constant bandgap (Mg) profile. Conversely, the constant profile case has voltage dependent current collection and Voc losses that become very pronounced as the interface state defect density is increased (compare with Figure 12, constant profile). The constant Mg profile in ZnMgO introduces secondary barrier when free carrier density is low under forward voltage (not shown, band diagram only shows V=0 case). Note that there is also a small barrier at the ZnO/ZnMgO interface when the ZnMgO free carrier density is high (see band diagram in Figure 13), that would not be present

with a Gaussian profile. However, voltage dependent current collection, without Voc loss is observed if we increase the peak energy in the Gaussian profile case (not shown).

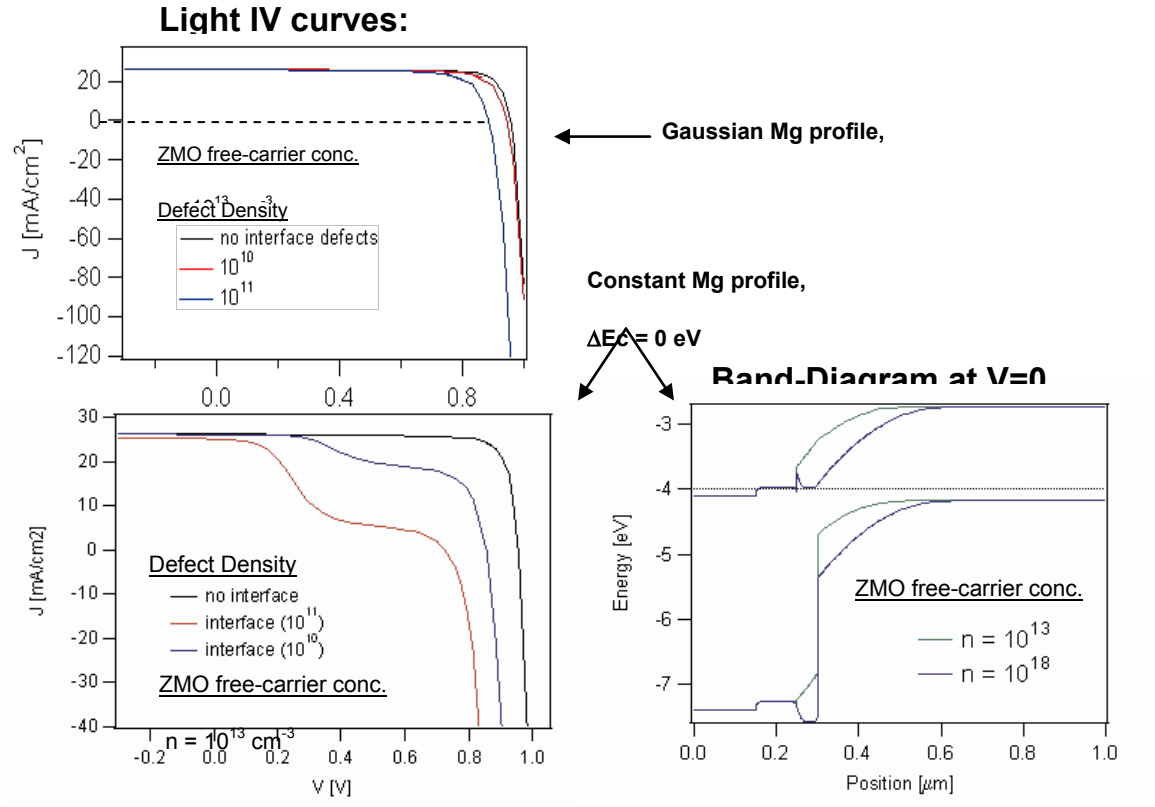

Figure 13 - Simulated device light IV curves (left) and band diagram (right) for constant ZnMgO bandgap, and 0 eV conduction band offset with mid-bandgap CIGS (bottom), and Gaussian ZnMgO profile.

In summary the modeling and simulation results indicate that the Gaussian profile with conduction band cliff at the interface is not detrimental as long as the free-carrier concentration is keep lower, and the Gaussian peak energy is not too high.

Conclusions

Incremental progress in the novel device performance was demonstrated throughout the program, and ultimately achieved performance results that exceeded the milestones ahead of schedule and set the stage for a follow-on incubator program. AST has successfully developed mid-bandgap CIGS based devices with metal-oxide buffer layers (no Cd) that match the average performance of the baseline low bandgap CIGS with CdS buffer layer small-area devices. Metal-oxide buffer layer devices with mid-bandgap CIGS alloys on polyimide substrates were produced with efficiencies of over 12%. Corresponding mid-bandgap devices with CdS buffers produced over 13% efficient devices. Furthermore, no obvious degradation in the device performance has been observed to date, after proper storage ambient of the different types of unencapsulated devices

were identified. It was also determined from a device emulation program that the non-uniform Mg profile in the APCVD grown ZnMgO was not necessarily detrimental to the ZnMgO/mid-bandgap CIGS performance as long as the Mg non-uniformity was not excessive and the ZnMgO free-carrier concentration was lower.

---

[1] J.D. Cohen, J. T. Heath, and W.N. Shafarman,"New Junction Capacitance Methods fo the Study of Defect Distributions and Carrier Properties in the Copper Indium Diselenide Alloys," Table 1, MRS Symposium Proceeding, Vol. 763, pp429-440, (2003).

[2] M. Gloeckler and J. Sites, "Efficiency limitations for wide-bandgap chalcopyrite solar cells," *Thin Solid Films*, v480-481, pp 241-245, (2005)

[3] T. Minemoto, et al., "Theoretical analysis of the effect of conduction band offset of window/CIS layers on performance of CIS solar cells using device simulation," *Sol. Energy Mat. & Sol. Cells*, 67, pp83-88, (2001).

[4] G. B. Turner, R.J. Schwartz, and J.L. Gray, "Band Discontinuity and Bulk vs. Interface Recombination in CdS/CuInSe2 Solar Cells," 20th IEEE PVSC, pp 1457 – 1460, (1988).

REPORT DOCUMENTATION PAGE

Form Approved
OMB No. 0704-0188

PLEASE DO NOT RETURN YOUR FORM TO THE ABOVE ORGANIZATION.

1. REPORT DATE *(DD-MM-YYYY)*	2. REPORT TYPE	3. DATES COVERED *(From - To)*
April 2011	Subcontract Report	10/26/09 - 10/26/10

4. TITLE AND SUBTITLE
ZnMgO by APCVD Enabling High-Performance Mid-bandgap CIGS on Polyimide Modules

5a. CONTRACT NUMBER
DE-AC36-08GO28308

5b. GRANT NUMBER

5c. PROGRAM ELEMENT NUMBER

6. AUTHOR(S)
Lawrence Woods

5d. PROJECT NUMBER
NREL/SR-5200-51379

5e. TASK NUMBER
PV10.1199

5f. WORK UNIT NUMBER

7. PERFORMING ORGANIZATION NAME(S) AND ADDRESS(ES)
Ascent Solar Technologies, Inc.
8120 Shaffer Pkwy.
Littleton, CO 80127

8. PERFORMING ORGANIZATION REPORT NUMBER
NEU-0-99010-02

9. SPONSORING/MONITORING AGENCY NAME(S) AND ADDRESS(ES)
National Renewable Energy Laboratory
1617 Cole Blvd.
Golden, CO 80401-3393

10. SPONSOR/MONITOR'S ACRONYM(S)
NREL

11. SPONSORING/MONITORING AGENCY REPORT NUMBER
NREL/SR-5200-51379

12. DISTRIBUTION AVAILABILITY STATEMENT
National Technical Information Service
U.S. Department of Commerce
5285 Port Royal Road
Springfield, VA 22161

13. SUPPLEMENTARY NOTES
NREL Technical Monitor: Brian Keyes

14. ABSTRACT *(Maximum 200 Words)*

This Pre-Incubator project was designed to increase the “real world” CIGS based photovoltaic module performance and decrease the Levelized Cost of Energy (LCOE) of systems utilizing those modules compared to our traditional CIGS based photovoltaic modules. This was enabled by a) increasing the CIGS bandgap and b) developing better matched device finishing layers to the mid-bandgap CIGS based photovoltaics; including window and buffer layers (and eventually the TCO). Incremental progress in the novel device performance was demonstrated throughout the program, and ultimately achieved performance results that exceeded the milestones ahead of schedule. Metal-oxide buffer layer devices with mid-bandgap CIGS alloys on polyimide substrates were produced with efficiencies of over 12%. Corresponding mid-bandgap devices with CdS buffers produced over 13% efficient devices. Furthermore, no obvious degradation in the device performance has been observed to date, after proper storage ambient of the different types of unencapsulated devices were identified.

15. SUBJECT TERMS
Photovoltaic; CIGS; polyimide

16. SECURITY CLASSIFICATION OF:			17. LIMITATION OF ABSTRACT	18. NUMBER OF PAGES	19a. NAME OF RESPONSIBLE PERSON
a. REPORT	b. ABSTRACT	c. THIS PAGE			19b. TELEPHONE NUMBER (*Include area code*)
Unclassified	Unclassified	Unclassified	UL		